

# Polymer-Based Thermally Stable Chemiresistive Sensor for Real-Time Monitoring of NO<sub>2</sub> Gas Emission

Geon Gug Yang,<sup>‡</sup> Dong-Ha Kim,<sup>‡</sup> Sanket Samal, Jungwoo Choi, Heejung Roh, Camille E. Cunin, Hyuck Mo Lee, Sang Ouk Kim,<sup>\*</sup> Mircea Dincă,<sup>\*</sup> and Aristide Gumyusenge<sup>\*</sup>



Cite This: *ACS Sens.* 2023, 8, 3687–3692



Read Online

ACCESS |



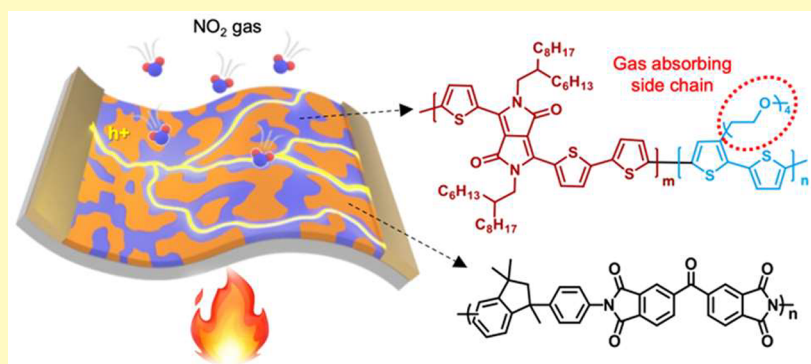
Metrics & More



Article Recommendations



Supporting Information



**ABSTRACT:** We present a thermally stable, mechanically compliant, and sensitive polymer-based NO<sub>2</sub> gas sensor design. Interconnected nanoscale morphology driven from spinodal decomposition between conjugated polymers tethered with polar side chains and thermally stable matrix polymers offers judicious design of NO<sub>2</sub>-sensitive and thermally tolerant thin films. The resulting chemiresistive sensors exhibit stable NO<sub>2</sub> sensing even at 170 °C over 6 h. Controlling the density of polar side chains along conjugated polymer backbone enables optimal design for coupling high NO<sub>2</sub> sensitivity, selectivity, and thermal stability of polymer sensors. Lastly, thermally stable films are used to implement chemiresistive sensors onto flexible and heat-resistant substrates and demonstrate a reliable gas sensing response even after 500 bending cycles at 170 °C. Such unprecedented sensor performance as well as environmental stability are promising for real-time monitoring of gas emission from vehicles and industrial chemical processes.

**KEYWORDS:** gas sensing, organic electronics, mixed conductors, polymer blends, thermal stability

Accurate and real-time monitoring of toxic gas emissions is crucial to mitigating potential health threats from increasing atmospheric pollution. In this regard, high performance, low-cost sensors for toxic gases are needed.<sup>1–4</sup> Until now, most gas sensor designs have relied on porous materials, 2D materials, and inorganic oxides as the sorbates for sensitive detection.<sup>5,6</sup> Unfortunately, those inorganic materials are hard to process into desired architectures in a cost-effective way, and the resulting devices are mechanically rigid and hence difficult to incorporate onto gas pipes and exhausts directly. Recently, conjugated polymers have garnered increasing attention as active materials for gas sensing, owing to their lightweight and mechanically flexible characteristics, highly desirable for facile system integration,<sup>7–9</sup> their high-performance sensing capabilities,<sup>10</sup> their facile chemical tunability for engineering device selectivity and sensitivity, as well as their solution-based processability, which is attractive for low manufacturing cost.<sup>11–14</sup> Conjugated polymers can be designed to bear abundant delocalized electrons along the  $\pi$  conjugation as well as polar side groups, allowing electrostatic

interactions with the industrial hazardous gases, typically polar small molecules (e.g., NO<sub>x</sub> and SO<sub>x</sub>).<sup>15–17</sup> This facilitates controllability of sorbate–analyte interaction and, thereby, eventual enhancement in sensing performances.

As most of the industrial emissions are generated from fossil fuel combustion, real-time monitoring of toxic gases inevitably requires operating under elevated temperature conditions. Ideally, monitoring of these gases should be implemented at smoke stack or exhaust pipe levels. There, the use of conjugated polymers is commonly challenging as their functionality tends to be vulnerable under such high temperature environments.<sup>18–21</sup> Polymer  $\pi$ – $\pi$  stacking, which is crucial to electrical conductivity, is greatly perturbed

**Received:** July 25, 2023

**Accepted:** September 14, 2023

**Published:** September 18, 2023



by the thermal fluctuations, leading to poor device performances.<sup>22,23</sup> Consequently, polymer-based gas sensors have been limited to temperatures below 100 °C.<sup>17</sup> To overcome inherent limitations related to extreme environments in polymer-based electronics, researchers typically employ molecular-level design and engineering strategies.<sup>24–29</sup> Notably, organic electronics based on polymer composites structures have been reported to sustain unusually high temperatures over 220 °C.<sup>30,31</sup> Among several strategies to form such composites, blending conjugated polymers with high glass-transition temperature (high  $T_g$ ) matrices has been demonstrated as a versatile and straightforward approach to combine environmental robustness with high electronic performance.<sup>29–31</sup> In such blends, interpenetrating spinodal-like morphologies between conjugated polymers and thermally stable matrices are used to effectively prevent the collapse of  $\pi$ - $\pi$  stacks between neighboring polymer chains and thus to retain electronic functionality at the elevated temperatures.

To deploy this composite strategy into gas sensors, one intriguing class of conjugated polymers is organic mixed ionic-electronic conductors (OMIECs).<sup>32,33</sup> Such polymers have been actively researched for organic electrochemical transistors (OECTs),<sup>33–35</sup> where the voltage-driven insertion of ionic species in the polymeric bulk modulates the channel conductance. Typically, these polymers are conjugated backbones tethered with the polar side chains for ionic insertion.<sup>35–41</sup> This chemical structure is also an advantageous platform for investigating molecular interactions between polymers and small-molecule analytes (e.g., toxic gases) as well as for scalable synthesis. Like other polymers mentioned above, these structures also suffer from poor environmental stability, including thermal stability. The common OMIECs are stable only up to 120 °C bakes,<sup>42,43</sup> with the recent exception of diketopyrrolopyrrole (DPP)-based OMIECs.<sup>44–46</sup> For instance, our group recently showed that with systematic control over the amount of polar side chains (triethylene glycol, TEG, which is known for enhancing gas affinity)<sup>15–17</sup> along the backbone, we can achieve optimal electrochemical modulation and unprecedented thermal stability (300 °C baking) in DPP copolymers.<sup>46</sup> Motivated by the chemically tunable affinity toward polar molecules in these DPP-based copolymers, as well as their thermal stability, we are intrigued by whether such OMIEC systems can be employed for sensing toxic gases (especially NO<sub>2</sub>) for real-time monitoring of industrial and domestic emissions.

In this work, we demonstrate a thermally stable and flexible NO<sub>2</sub> gas sensor using blend composites of a DPP-based OMIEC and a polyimide matrix. We form a spinodal-like morphology between the mixed conductor and the high  $T_g$  matrix to synergistically combine high affinity toward NO<sub>2</sub> as well as high-temperature operation stability. The blend system is readily solution-processable into thin films, thus facilitating the fabrication of chemiresistive sensing devices, even onto flexible substrates. Chemiresistive NO<sub>2</sub> gas sensors with excellent response values, low detection limit, high selectivity, and long-term stability even in the temperature range, such as those found in exhaust pipes, are thus presented. The composite design we report showed one of the best NO<sub>2</sub> detection performances to date, and the flexible device architecture we employ demonstrated potential integration into exhaust pipes and chimneys. This work thus demonstrates both the importance of structural design of new sensing

materials, especially conjugate polymers, and promising device architectures for integrated monitoring of toxic gases.

To combine efficient gas absorption and thermal stability, we designed an active channel comprised of a blend system between a semiconducting polymer (DPP-30gT) and a high  $T_g$  and hence morphology stabilizing matrix, herein Matrimid (MI). Figure 1a illustrates the studied architecture of a gas

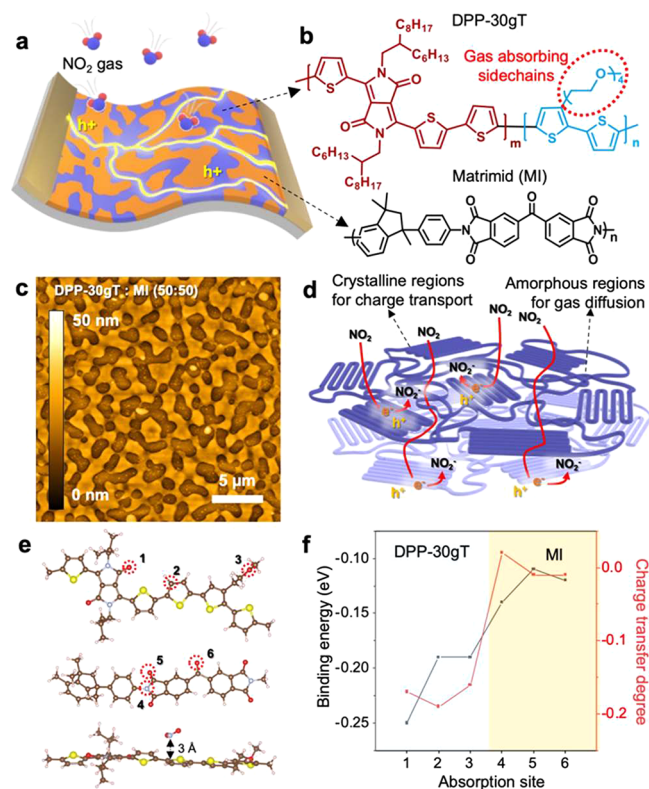


**Figure 1.** Design of a thermally stable chemiresistive sensor for real-time monitoring of NO<sub>2</sub> emission. (a) Illustration of a gas sensor design based on semiconducting polymer composites. (b) Chemical structures of DPP-30gT and Matrimid. (c) AFM height image of the blend film. (d) Illustration of the proposed NO<sub>2</sub> sensing mechanism. (e, f) Proposed NO<sub>2</sub> absorption sites and respective calculated binding energies with the DPP-30gT:MI blend system.

sensor, where the active channel is a blend composite made of a DPP-30gT copolymer and MI (Figure 1b). The semiconductive DPP-30gT, serving as the active material for NO<sub>2</sub> gas absorption, was used to form a bicontinuous morphology across the film with the thermally stable MI ( $T_g \sim 325$  °C). The matrix polymer surrounds the semiconducting domains and enables the overall environmental and thermal robustness (Figures 1c and S1) in accordance with previous works.<sup>30</sup> Our previous works have shown that, though beneficial for electrochemical activity, the increased density of polar side chains deters the electronic properties in mixed conducting copolymers.<sup>46,47</sup> We thus selected DPP-30gT to endow the sensor channel with (i) sufficient affinity toward NO<sub>2</sub> molecules, (ii) a semicrystalline morphology promoting facile diffusion, and (iii) sufficient electronic charge transport needed to record the chemiresistive sensor response (Figure 1d). To control the blend morphology, we varied the compositional ratio between DPP-30gT and MI between 0 and 100 wt % MI. Upon rapid evaporation of a common solvent during the spin coating, a spinodal-like interpenetrating morphology between

the two components at 1:1 ratio was triggered (Figure S1). We hypothesize that once this interpenetrating morphology is formed, the high  $T_g$  matrix polymer will effectively suppress the thermal fluctuations within the blend film, particularly when the films are heated below its  $T_g$  (Figure S2),<sup>30,31</sup> and thus allow stable sensing performance even at elevated temperature.

To understand the sensing mechanism in our polymer system, we first used Raman spectroscopy to evaluate the chemical interaction between the polymer system and  $\text{NO}_2$ . There was no specific peak shift in the DPP-30gT spectrum before and after  $\text{NO}_2$  exposure (Figure S3a), indicative of no specific binding between DPP-30gT and  $\text{NO}_2$ . This behavior agrees with previous reports using conjugated polymers for  $\text{NO}_2$  gas sensing, where the gas molecules have been shown to simply function as dopants, thus changing the conductance of the semiconducting polymer during exposure.<sup>15–17</sup> We also calculated the binding energy and charge transfer level around all possible absorption sites in the blend system and further confirmed the lack of specific bonding between the polymers and  $\text{NO}_2$  (Figure 1e and f). Our simulations accounted for all potential binding positions in accordance with previous reports but simplified the system as one repeat unit with a shortened side chain.<sup>15</sup> In a fully relaxed state, the  $\text{NO}_2$  molecules were found to equilibrate around each site at distances over 3 Å. In the case of bond forming interactions, distances under 2 Å are expected. As shown in Figure 1f, the binding energy and charge transfer degree were greatest around the conjugated polymer compared to the matrix, which means that the insulating polymer mostly acts as a rigidifying host and does not contribute to molecular adsorption. These computation results thus supported the Raman results that  $\text{NO}_2$  gas simply acts as a doping gas without any specific bonding. Note that our simulations do not capture the entire polymer system including  $\pi$ - $\pi$  stacking of polymer chains, long alkyl chains, TEG side chains, and potential sites obstructed by the  $\pi$ - $\pi$  stacking in a real polymer crystallite morphology.<sup>15</sup> Nonetheless we anticipate that the porous nature of our blends would facilitate the  $\text{NO}_2$  diffusion, thus enhancing the device sensitivity, as illustrated in Figure 1d.

With this operating mechanism, the sensitivity of our polymer channel would depend on its ability to attract  $\text{NO}_2$  molecules into the bulk, i.e., the doping level of the semiconducting component. We thus evaluated this doping capability of  $\text{NO}_2$  toward DPP-30gT using field-effect transistor devices (Figure S3b). Upon exposure to  $\text{NO}_2$  gas, the source-drain current showed to increase, indicative of channel doping. We also used the unfunctionalized DPP analogue (no TEG side chains, DPP-0gT) to show that without the TEG groups in the polymer structure, only a slight change in the current is detected (Figure S3c). The less hydrophilic DPP-0gT does not efficiently uptake the polar  $\text{NO}_2$  molecules, thus underscoring the importance of the side chains on the sensitivity of the sensor. Note that this shift in the drain current was attainable in a bottom-contact device configuration (where the current is measured at the bottom interface). This was more indirect evidence that the active material in our sensor allows effective diffusion of  $\text{NO}_2$  molecules into the bulk as illustrated in Figure 1d, a property that is enabled herein by both the presence of polar pendant groups as well as amorphous domains within the film bulk. We could thus deduce that, with the presence of TEG side chains,  $\text{NO}_2$  gas is attracted toward the polymer backbone and easily abducts the electron from the latter, thus generating mobile

holes which translate into a greater electrical conductivity in the device channel.<sup>15–17</sup> It is thus implied that semicrystalline films are preferred here (given that the electronic performance is retained, which is the case for DPP-30gT)<sup>46</sup> as the amorphous regions within the active sensing area will facilitate the diffusion of gas molecules into the film bulk (Figure 1d).<sup>6,16</sup>

We then fabricated chemiresistive-type sensors and evaluated the  $\text{NO}_2$  gas sensing properties of the DPP-30gT:MI blends. More details regarding the lab-made gas measurement setup and the fabrication steps of the gas sensing devices can be found in the Experimental details section in the Supporting Information. Note that all the sensing measurements were conducted under dry air conditions (1.5% relative humidity), and the sensing response is determined by measuring the difference in channel resistance when  $\text{NO}_2$  gas is present and when it is absent ( $R_{\text{air}}/R_{\text{gas}}$ ). We primarily assessed the chemiresistors' sensing performance based on sensitivity, selectivity, reversibility, and operational stability, especially at elevated temperatures. We thus measured the sensing performance within a temperature range of 60 to 170 °C, a range similar to the conditions found in exhaust pipes and chimneys. Figure 2a shows the dynamic response of our sensor to 1 ppm of  $\text{NO}_2$  at different temperatures indicating high sensitivity of the DPP-30gT:MI channel toward  $\text{NO}_2$  gas across a wide range of heating conditions. Due to the thermally promoted hopping of charge carriers in the polymer channel,<sup>30</sup> the sensors showed enhanced performance with increasing

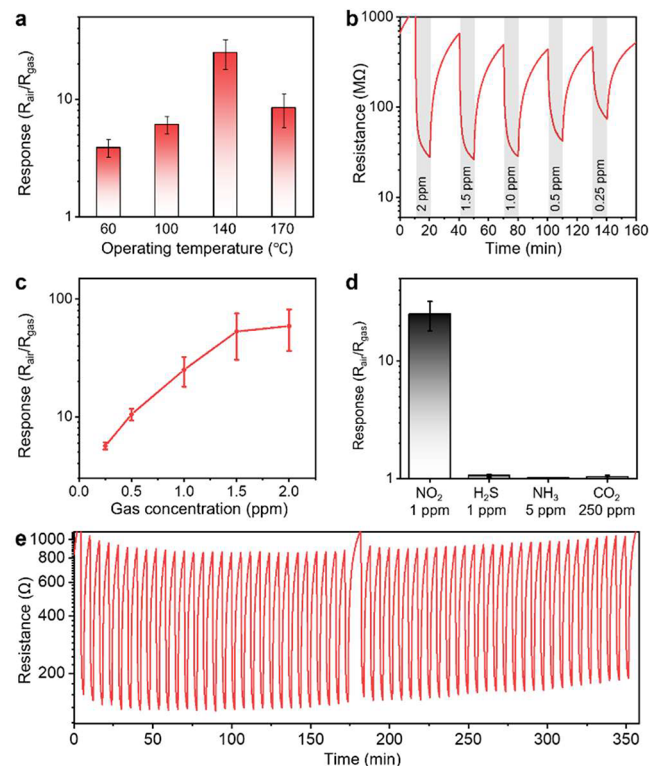


**Figure 2.**  $\text{NO}_2$  sensing performance of chemiresistors based on DPP-30gT:MI. (a) Response values of DPP-30gT:MI toward 1 ppm of  $\text{NO}_2$  at various operating temperatures. (b, c) Dynamic resistance changes in the DPP-30gT:MI channel toward 2–0.25 ppm of  $\text{NO}_2$  gas at 140 °C. (d) Selectivity tests of  $\text{NO}_2$ ,  $\text{H}_2\text{S}$ ,  $\text{NH}_3$ , and  $\text{CO}_2$ . (e) Long-term cycling (58 cycles, >6 h) stability tests of DPP-30gT:MI sensors at 170 °C.

temperature and showed optimal response around 140 °C. Excessive heating (above 170 °C) was found to be detrimental to the sensors response as evidenced by a decline in charge transport characteristics as well as the loss in molecular-level order (Figure S4). We thus set ~140–170 °C as the optimal operating temperature for our blend system. Among polymer-based sensors to date, this is over 70 °C higher than the best achievable temperature for NO<sub>2</sub> sensing,<sup>17</sup> promising potential for real-time and integrated (at the exhausts level) monitoring of emitted gas in industrial and residential setups. Additionally, at such temperatures, the DPP-30gT:MI-based sensors exhibit a dynamic response toward varying the gas concentration (2 to 0.25 ppm at 140 °C) (Figure 2b, c). Even at extremely low NO<sub>2</sub> concentrations (0.25 ppm), the sensors could yield dynamic responses as high as 5.7, which is desirable for practical use. The blend-based sensors also showed a response time of 1.5 min, which is among the fastest polymer-based NO<sub>2</sub> sensors (Figure S5).<sup>15–17</sup> This level of sensitivity was also accompanied by excellent selectivity toward NO<sub>2</sub> versus other common small molecule gases. In polymer-based sensors, it is often challenging to differentiate between common gases such as NO<sub>2</sub>, H<sub>2</sub>S, NH<sub>3</sub>, and CO<sub>2</sub>.<sup>17,48–50</sup> As shown in Figure 2d, DPP-30gT:MI-based sensors exhibits excellent selectivity toward NO<sub>2</sub> gas ( $R_{\text{air}}/R_{\text{gas}} \sim 25.04$  @ 1 ppm) compared to H<sub>2</sub>S ( $R_{\text{air}}/R_{\text{gas}} \sim 1.06$  @ 1 ppm), NH<sub>3</sub> ( $R_{\text{air}}/R_{\text{gas}} \sim 1.01$  @ 5 ppm), and CO<sub>2</sub> ( $R_{\text{air}}/R_{\text{gas}} \sim 1.04$  @ 250 ppm), with a cross-selectivity value ( $R_{\text{NO}_2}/R_{\text{inter}} > 23.62$ , where  $R_{\text{NO}_2}$  and  $R_{\text{inter}}$  denote the response toward NO<sub>2</sub> and interfering gases, respectively).<sup>17</sup> Such sensitivity, selectivity, and response speeds under trace amounts (sub-ppm) of gas molecules showed potential feasibility for environmental monitoring applications using polymer-based sensors.

We then sought to evaluate the feasibility of integrating our sensor devices into real-world scenarios (e.g., pipes and chimneys) by fabricating fully flexible devices and monitoring their performance under both extreme temperatures and bending radius. Given the facile processability of the studied all-polymer active material, we could readily cast DPP-30gT:MI blends onto prepatterned polyimide substrates (Figure 3a). We then evaluated the gas sensing performances under four different measurement scenarios: (i) flat state, (ii) bent state, (iii) flat state after 100 bending cycles, and (iv) flat state after 500 bending cycles (Figure 3b, c). The flexible sensors exhibited stable and reversible sensing performances in both flat and bent states. Even after 500 bending cycles, the sensors maintained stable and reversible response as shown during 6 cyclic exposures to 1 ppm gas (Figure 3c). This mechanical endurance was also concomitant with tolerance versus extreme temperatures. For instance, after subjecting the flexible sensor to 500 bending cycles, we brought the operating temperature to 170 °C, emulating real-world scenarios (Figure 3d), and probed the performance toward low (1 ppm) NO<sub>2</sub> concentrations. As shown in Figure 3e, the DPP-30gT:MI-based sensors exhibit robust sensing capabilities. Despite the slight downward drift in the baseline resistance over time, stable and reversible sensing behaviors occurred after subjecting our sensors to both mechanical and thermal stress. This level of tolerance to harsh conditions is highly desirable for the real-time monitoring of gas emissions using polymer-based sensors. Upon surveying the literature (Table S1 and Figure S6), the sensitivity levels found in DPP-30gT:MI blends toward NO<sub>2</sub> gas especially at such elevated temperatures were unprecedented, thus promising future polymer-based sensors.

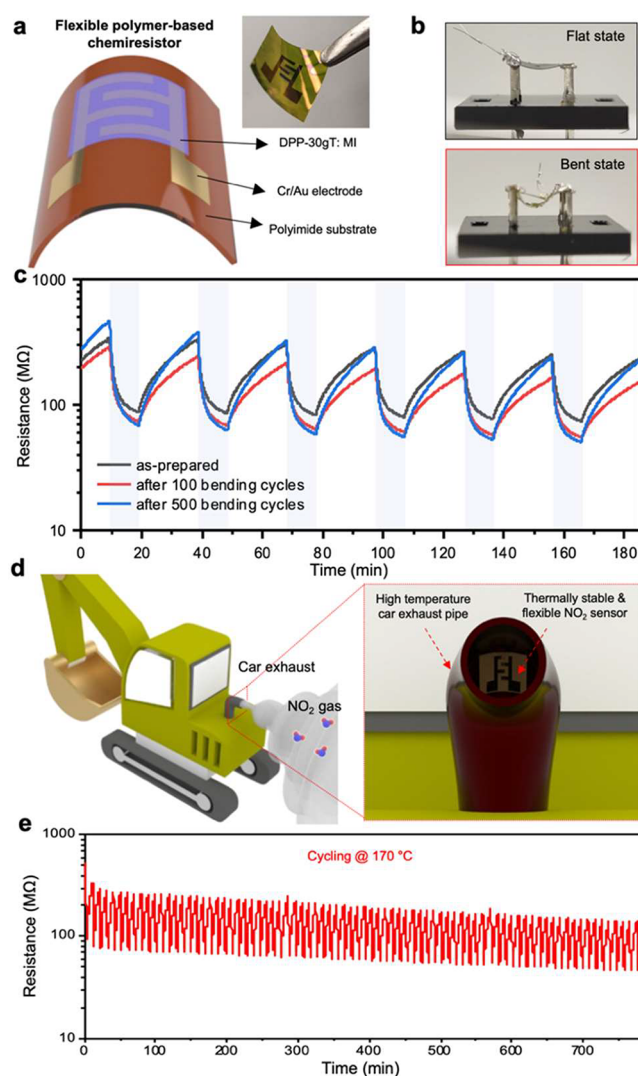


**Figure 3.** Demonstration of a thermally stable and mechanically flexible sensor for real-time monitoring of NO<sub>2</sub>. (a) Illustrations of flexible polymer chemiresistor based on a polyimide substrate. (b) Photograph of sensors in flat and bent states. (c) Dynamic resistance transitions of sensors in flat and bent states upon exposure to 1 ppm of NO<sub>2</sub> gas at 140 °C before repeated flexing. (d) Illustration of the thermally stable and flexible NO<sub>2</sub> chemiresistor attached onto a car exhaust pipe. (e) Long-cycling stability tests of DPP-30gT:MI-based sensors after 500 bending cycles at 170 °C.

To summarize, we have presented a thermally stable NO<sub>2</sub> gas sensor enabled by a judicious composite design composed of a polymer mixed conductor and a thermally robust matrix. The insulating matrix could effectively suppress the thermal fluctuations of the NO<sub>2</sub>-affine semiconductor, resulting in stable sensing performance even at elevated temperatures above 170 °C over 6 h. Moreover, the blend system we studied showed an extremely high sensing response due to not only the chemically engineered binding sites for polar NO<sub>2</sub> gas, but also the systematic balance of amorphous regions within the sensing volume to further boost the NO<sub>2</sub> gas diffusion into the bulk film. Finally, typical solution processing of the blend composites onto flexible and heat resistant substrates allowed us to demonstrate reliable gas sensing performance even under severe mechanical bending. We anticipate that the structurally controllable response to various analytes available in this class

of polymers, as well as their thermal stabilization through polymer blending, can serve as a valuable platform for designing a real-time monitor for toxic gases.

## ■ ASSOCIATED CONTENT

### SI Supporting Information

The Supporting Information is available free of charge at <https://pubs.acs.org/doi/10.1021/acssensors.3c01530>.

Experimental details and supporting data (materials, transistor fabrication and characterization, thin film morphology and spectroscopy measurement details, computation and simulation details, gas sensor fabrication and measurement setup), supporting figures and table, and supporting references (PDF)

## ■ AUTHOR INFORMATION

### Corresponding Authors

**Sang Ouk Kim** – Department of Materials Science and Engineering, Korea Advanced Institute of Science and Technology (KAIST), Daejeon 34141, Korea; Email: [sangouk.kim@kaist.ac.kr](mailto:sangouk.kim@kaist.ac.kr)

**Mircea Dincă** – Department of Chemistry, Massachusetts Institute of Technology, Cambridge, Massachusetts 02139, United States; Email: [mdinca@mit.edu](mailto:mdinca@mit.edu)

**Aristide Gumyusenge** – Department of Materials Science and Engineering, Massachusetts Institute of Technology, Cambridge, Massachusetts 02139, United States; [orcid.org/0000-0003-4995-5222](https://orcid.org/0000-0003-4995-5222); Email: [aristide@mit.edu](mailto:aristide@mit.edu)

### Authors

**Geon Gug Yang** – Department of Materials Science and Engineering, Massachusetts Institute of Technology, Cambridge, Massachusetts 02139, United States; Department of Materials Science and Engineering, Korea Advanced Institute of Science and Technology (KAIST), Daejeon 34141, Korea

**Dong-Ha Kim** – Department of Chemistry, Massachusetts Institute of Technology, Cambridge, Massachusetts 02139, United States

**Sanket Samal** – Department of Materials Science and Engineering, Massachusetts Institute of Technology, Cambridge, Massachusetts 02139, United States

**Jungwoo Choi** – Department of Materials Science and Engineering, Korea Advanced Institute of Science and Technology (KAIST), Daejeon 34141, Korea; [orcid.org/0000-0003-3988-6331](https://orcid.org/0000-0003-3988-6331)

**Heejung Roh** – Department of Materials Science and Engineering, Massachusetts Institute of Technology, Cambridge, Massachusetts 02139, United States

**Camille E. Cunin** – Department of Materials Science and Engineering, Massachusetts Institute of Technology, Cambridge, Massachusetts 02139, United States

**Hyuck Mo Lee** – Department of Materials Science and Engineering, Korea Advanced Institute of Science and Technology (KAIST), Daejeon 34141, Korea; [orcid.org/0000-0003-4556-6692](https://orcid.org/0000-0003-4556-6692)

Complete contact information is available at:

<https://pubs.acs.org/doi/10.1021/acssensors.3c01530>

### Author Contributions

<sup>‡</sup>G.G.Y. and D.-H.K. contributed equally to this work.

## Funding

G.G.Y. was supported by the National Creative Research Initiative (CRI) Center for Multi-Dimensional Directed Nanoscale Assembly (2015R1A3A2033061), National Research Foundation of Korea (NRF) funded by the Ministry of Science. D.-H.K. and M.D. acknowledge the support from the U.S. Department of Energy (DE-SC0023288).

## Notes

The authors declare no competing financial interest.

## ■ REFERENCES

- (1) Schroeder, V.; Savagatrup, S.; He, M.; Lin, S.; Swager, T. M. Carbon Nanotube Chemical Sensors. *Chem. Rev.* **2019**, *119*, 599–663.
- (2) Meng, Z.; Stolz, R. M.; Mendecki, L.; Mirica, K. A. Electrically-Transduced Chemical Sensors Based on Two-Dimensional Nanomaterials. *Chem. Rev.* **2019**, *119*, 478–598.
- (3) Li, H.; Shi, W.; Song, J.; Jang, H.-J.; Dailey, J.; Yu, J.; Katz, H. E. Chemical and Biomolecule Sensing with Organic Field-Effect Transistors. *Chem. Rev.* **2019**, *119*, 3–35.
- (4) Zhou, X.; Lee, S.; Xu, Z.; Yoon, J. Recent Progress on the Development of Chemosensors for Gases. *Chem. Rev.* **2015**, *115*, 7944–8000.
- (5) Choi, S. J.; Kim, I. D. Recent Developments in 2D Nanomaterials for Chemiresistive-Type Gas Sensors. *Electron. Mater. Lett.* **2018**, *14*, 221–260.
- (6) Lee, J.-H. Gas Sensors Using Hierarchical and Hollow Oxide Nanostructures: Overview. *Sens. Actuators B Chem.* **2009**, *140*, 319–336.
- (7) McQuade, D. T.; Pullen, A. E.; Swager, T. M. Conjugated Polymer-Based Chemical Sensors. *Chem. Rev.* **2000**, *100*, 2537–2574.
- (8) Tajik, S.; Beitollahi, H.; Nejad, F. G.; Dourandish, Z.; Khalilzadeh, M. A.; Jang, H. W.; Venditti, R. A.; Varma, R. S.; Shokouhimehr, M. Recent Developments in Polymer Nanocomposite-Based Electrochemical Sensors for Detecting Environmental Pollutants. *Ind. Eng. Chem. Res.* **2021**, *60*, 1112–1136.
- (9) Ma, Z.; Chen, P.; Cheng, W.; Yan, K.; Pan, L.; Shi, Y.; Yu, G. Highly Sensitive, Printable Nanostructured Conductive Polymer Wireless Sensor for Food Spoilage Detection. *Nano Lett.* **2018**, *18*, 4570–4575.
- (10) Zhang, X.; Wang, B.; Huang, L.; Huang, W.; Wang, Z.; Zhu, W.; Chen, Y.; Mao, Y. L.; Facchetti, A.; Marks, T. J. Breath Figure-Derived Porous Semiconducting Films for Organic Electronics. *Sci. Adv.* **2020**, *6*, eaaz1042.
- (11) Janata, J.; Josowicz, M. Conducting Polymers in Electronic Chemical Sensors. *Nat. Mater.* **2003**, *2*, 19–24.
- (12) Cichosz, S.; Masek, A.; Zaborski, M. Polymer-Based Sensors: A Review. *Polym. Test.* **2018**, *67*, 342–348.
- (13) Liu, X.; Zheng, W.; Kumar, R.; Kumar, M.; Zhang, J. Conducting Polymer-Based Nanostructures for Gas Sensors. *Coord. Chem. Rev.* **2022**, *462*, 214517.
- (14) Ma, Z.; Shi, W.; Yan, K.; Pan, L.; Yu, G. Doping Engineering of Conductive Polymer Hydrogels and Their Application in Advanced Sensor Technologies. *Chem. Sci.* **2019**, *10*, 6232–6244.
- (15) Kang, Y.; Kwak, D. H.; Kwon, J. E.; Kim, B.-G.; Lee, W. H. NO<sub>2</sub>-Affinitive Conjugated Polymer for Selective Sub-Parts-Per-Billion NO<sub>2</sub> Detection in a Field-Effect Transistor Sensor. *ACS Appl. Mater. Interfaces* **2021**, *13*, 31910–31918.
- (16) Chae, H.; Han, J. M.; Ahn, Y.; Kwon, J. E.; Lee, W. H.; Kim, B.-G. NO<sub>2</sub>-Affinitive Amorphous Conjugated Polymer for Field-Effect Transistor Sensor toward Improved NO<sub>2</sub> Detection Capability. *Adv. Mater. Technol.* **2021**, *6*, 2100580.
- (17) Park, H.; Kim, D.-H.; Ma, B. S.; Shin, E.; Kim, Y.; Kim, T.-S.; Kim, F. S.; Kim, I.-D.; Kim, B. J. High-Performance, Flexible NO<sub>2</sub> Chemiresistors Achieved by Design of Imine-Incorporated n-Type Conjugated Polymers. *Adv. Sci.* **2022**, *9*, 2200270.
- (18) Zhao, Y.; Zhao, X.; Rodgers, M.; Gumyusenge, A.; Ayzner, A. L.; Mei, J. Melt-Processing of Complementary Semiconducting Polymer

- Blends for High Performance Organic Transistors. *Adv. Mater.* **2017**, *29*, 1605056.
- (19) Sekitani, T.; Iba, S.; Kato, Y.; Someya, T. Pentacene Field-Effect Transistors on Plastic Films Operating at High Temperature above 100°C. *Appl. Phys. Lett.* **2004**, *85*, 3902.
- (20) Fan, Z.-P.; Li, X.-Y.; Purdum, G. E.; Hu, C.-X.; Fei, X.; Shi, Z.-F.; Sun, C.-L.; Shao, X.; Loo, Y.-L.; Zhang, H.-L. Enhancing the Thermal Stability of Organic Field-Effect Transistors by Electrostatically Interlocked 2D Molecular Packing. *Chem. Mater.* **2018**, *30*, 3638–3642.
- (21) Gumyusenge, A.; Mei, J. High Temperature Organic Electronics. *MRS Adv.* **2020**, *5*, 505–513.
- (22) Tashiro, K.; Ono, K.; Minagawa, Y.; Kobayashi, M.; Kawai, T.; Yoshino, K. Structure and Thermochromic Solid-State Phase Transition of Poly (3-Alkylthiophene). *J. Polym. Sci. B Polym. Phys.* **1991**, *29*, 1223–1233.
- (23) Joshi, S.; Pingel, P.; Grigorian, S.; Panzner, T.; Pietsch, U.; Neher, D.; Forster, M.; Scherf, U. Bimodal Temperature Behavior of Structure and Mobility in High Molecular Weight P3HT Thin Films. *Macromolecules* **2009**, *42*, 4651–4660.
- (24) Xu, J.; Wang, S.; Wang, G. J. N.; Zhu, C.; Luo, S.; Jin, L.; Gu, X.; Chen, S.; Feig, V. R.; To, J. W. F.; Rondeau-Gagné, S.; Park, J.; Schroeder, B. C.; Lu, C.; Oh, J. Y.; Wang, Y.; Kim, Y. H.; Yan, H.; Sinclair, R.; Zhou, D.; Xue, G.; Murmann, B.; Linder, C.; Cai, W.; Tok, J. B. H.; Chung, J. W.; Bao, Z. Highly Stretchable Polymer Semiconductor Films through the Nanoconfinement Effect. *Science* **2017**, *355*, 59–64.
- (25) Tran, D. T.; Gumyusenge, A.; Luo, X.; Roders, M.; Yi, Z.; Ayzner, A. L.; Mei, J. Effects of Side Chain on High Temperature Operation Stability of Conjugated Polymers. *ACS Appl. Polym. Mater.* **2020**, *2*, 91–97.
- (26) Griffini, G.; Douglas, J. D.; Piliago, C.; Holcombe, T. W.; Turri, S.; Fréchet, J. M. J.; Mynar, J. L. Long-Term Thermal Stability of High-Efficiency Polymer Solar Cells Based on Photocrosslinkable Donor-Acceptor Conjugated Polymers. *Adv. Mater.* **2011**, *23*, 1660–1664.
- (27) Seifrid, M.; Ford, M. J.; Li, M.; Koh, K. M.; Trefonas, P.; Bazan, G. C. Electrical Performance of a Molecular Organic Semiconductor under Thermal Stress. *Adv. Mater.* **2017**, *29*, 1605511.
- (28) Ke, Z.; You, L.; Tran, D. T.; He, J.; Perera, K.; Gumyusenge, A.; Mei, J. Thermally Stable and Solvent-Resistant Conductive Polymer Composites with Cross-Linked Siloxane Network. *ACS Appl. Polym. Mater.* **2021**, *3*, 1537–1543.
- (29) Lee, E. K.; Lee, M. Y.; Park, C. H.; Lee, H. R.; Oh, J. H. Toward Environmentally Robust Organic Electronics: Approaches and Applications. *Adv. Mater.* **2017**, *29*, 1703638.
- (30) Gumyusenge, A.; Tran, D. T.; Luo, X.; Pitch, G. M.; Zhao, Y.; Jenkins, K. A.; Dunn, T. J.; Ayzner, A. L.; Savoie, B. M.; Mei, J. Semiconducting Polymer Blends That Exhibit Stable Charge Transport at High Temperatures. *Science* **2018**, *362*, 1131–1134.
- (31) Gumyusenge, A.; Luo, X.; Ke, Z.; Tran, D. T.; Mei, J. Polyimide-Based High-Temperature Plastic Electronics. *ACS Mater. Lett.* **2019**, *1*, 154–157.
- (32) Paulsen, B. D.; Tybrandt, K.; Stavrinidou, E.; Rivnay, J. Organic Mixed Ionic-Electronic Conductors. *Nat. Mater.* **2020**, *19*, 13–26.
- (33) Tan, S. T. M.; Gumyusenge, A.; Quill, T. J.; LeCroy, G. S.; Bonacchini, G. E.; Denti, I.; Salleo, A. Mixed Ionic-Electronic Conduction, a Multifunctional Property in Organic Conductors. *Adv. Mater.* **2022**, *34*, 2110406.
- (34) Huang, W.; Chen, J.; Yao, Y.; Zheng, D.; Ji, X.; Feng, L. W.; Moore, D.; Glavin, N. R.; Xie, M.; Chen, Y.; Pankow, R. M.; Surendran, A.; Wang, Z.; Xia, Y.; Bai, L.; Rivnay, J.; Ping, J.; Guo, X.; Cheng, Y.; Marks, T. J.; Facchetti, A. Vertical Organic Electrochemical Transistors for Complementary Circuits. *Nature* **2023**, *613*, 496–502.
- (35) Li, P.; Lei, T. Molecular Design Strategies for High-Performance Organic Electrochemical Transistors. *J. Polym. Sci.* **2022**, *60*, 377–392.
- (36) Giovannitti, A.; Maria, I. P.; Hanifi, D.; Donahue, M. J.; Bryant, D.; Barth, K. J.; Makdah, B. E.; Savva, A.; Moia, D.; Zetek, M. M.; Barnes, P. R. F.; Reid, O. G.; Inal, S.; Rumbles, G.; Malliaras, G. G.; Nelson, J.; Rivnay, J.; McCulloch, I. The Role of the Side Chain on the Performance of N-Type Conjugated Polymers in Aqueous Electrolytes. *Chem. Mater.* **2018**, *30*, 2945–2953.
- (37) Hallani, R. K.; Paulsen, B. D.; Petty, A. J.; Sheelamantula, R.; Moser, M.; Thorley, K. J.; Sohn, W.; Rashid, R. B.; Savva, A.; Moro, S.; Parker, J. P.; Drury, O.; Alsufyani, M.; Neophytou, M.; Kosco, J.; Inal, S.; Costantini, G.; Rivnay, J.; McCulloch, I. Regiochemistry-Driven Organic Electrochemical Transistor Performance Enhancement in Ethylene Glycol-Functionalized Polythiophenes. *J. Am. Chem. Soc.* **2021**, *143*, 11007–11018.
- (38) Surgailis, J.; Savva, A.; Druet, V.; Paulsen, B. D.; Wu, R.; Hamidi-Sakr, A.; Ohayon, D.; Nikiforidis, G.; Chen, X.; McCulloch, I.; Rivnay, J.; Inal, S. Mixed Conduction in an N-Type Organic Semiconductor in the Absence of Hydrophilic Side-Chains. *Adv. Funct. Mater.* **2021**, *31*, 2010165.
- (39) Savva, A.; Hallani, R.; Cendra, C.; Surgailis, J.; Hidalgo, T. C.; Wustoni, S.; Sheelamantula, R.; Chen, X.; Kirkus, M.; Giovannitti, A.; Salleo, A.; McCulloch, I.; Inal, S. Balancing Ionic and Electronic Conduction for High-Performance Organic Electrochemical Transistors. *Adv. Funct. Mater.* **2020**, *30*, 1907657.
- (40) Roh, H.; Cunin, C.; Samal, S.; Gumyusenge, A. Towards Organic Electronics That Learn at the Body-Machine Interface: A Materials Journey. *MRS Commun.* **2022**, *12*, 565–577.
- (41) Nielsen, C. B.; Giovannitti, A.; Sbircea, D. T.; Bandiello, E.; Niazi, M. R.; Hanifi, D. A.; Sessolo, M.; Amassian, A.; Malliaras, G. G.; Rivnay, J.; McCulloch, I. Molecular Design of Semiconducting Polymers for High-Performance Organic Electrochemical Transistors. *J. Am. Chem. Soc.* **2016**, *138*, 10252–10259.
- (42) Melianas, A.; Quill, T. J.; LeCroy, G.; Tuchman, Y.; Loo, H. v.; Keene, S. T.; Giovannitti, A.; Lee, H. R.; Maria, I. P.; McCulloch, I.; Salleo, A. Temperature-Resilient Solid-State Organic Artificial Synapses for Neuromorphic Computing. *Sci. Adv.* **2020**, *6*, eabb2958.
- (43) Rivnay, J.; Inal, S.; Collins, B. A.; Sessolo, M.; Stavrinidou, E.; Strakosas, X.; Tassone, C.; Delongchamp, D. M.; Malliaras, G. G. Structural Control of Mixed Ionic and Electronic Transport in Conducting Polymers. *Nat. Commun.* **2016**, *7*, 1–9.
- (44) Krauss, G.; Meichsner, F.; Hochgesang, A.; Mohanraj, J.; Salehi, S.; Schmode, P.; Thelakkat, M. Polydiketopyrrolopyrroles Carrying Ethylene Glycol Substituents as Efficient Mixed Ion-Electron Conductors for Biocompatible Organic Electrochemical Transistors. *Adv. Funct. Mater.* **2021**, *31*, 2010048.
- (45) Chen, J.; Huang, W.; Zheng, D.; Xie, Z.; Zhuang, X.; Zhao, D.; Chen, Y.; Su, N.; Chen, H.; Pankow, R. M.; Gao, Z.; Yu, J.; Guo, X.; Cheng, Y.; Strzalka, J.; Yu, X.; Marks, T. J.; Facchetti, A. Highly Stretchable Organic Electrochemical Transistors with Strain-Resistant Performance. *Nat. Mater.* **2022**, *21*, 564–571.
- (46) Samal, S.; Roh, H.; Cunin, C. E.; Yang, G. G.; Gumyusenge, A. Molecularly Hybridized Conduction in DPP-Based Donor-Acceptor Copolymers toward High-Performance Iono-Electronics. *Small* **2023**, *19*, 2207554.
- (47) Roh, H.; Yue, S.; Hu, H.; Chen, K.; Kulik, H. J.; Gumyusenge, A. Unraveling Polymer-Ion Interactions in Electrochromic Polymers for Their Implementation in Organic Electrochemical Synaptic Devices. *Adv. Funct. Mater.* **2023**, 2304893.
- (48) Navale, S. T.; Mane, A. T.; Chougule, M. A.; Sakhare, R. D.; Nalage, S. R.; Patil, V. B. Highly Selective and Sensitive Room Temperature NO<sub>2</sub> Gas Sensor Based on Polypyrrole Thin Films. *Synth. Met.* **2014**, *189*, 94–99.
- (49) Kailasa, S.; Sai Bhargava Reddy, M.; Geeta Rani, B.; Maseed, H.; Venkateswara Rao, K. Twisted Polyaniline Nanobelts @ RGO for Room Temperature NO<sub>2</sub> Sensing. *Mater. Lett.* **2019**, *257*, 126687.
- (50) Bandgar, D. K.; Navale, S. T.; Mane, A. T.; Gupta, S. K.; Aswal, D. K.; Patil, V. B. Ammonia Sensing Properties of Polyaniline/ $\alpha$ -Fe<sub>2</sub>O<sub>3</sub> Hybrid Nanocomposites. *Synth. Met.* **2015**, *204*, 1–9.